INTERNATIONAL JOURNAL FOR NUMERICAL METHODS IN FLUIDS, VOL. 20, 649–662 (1995)

AN APPLICATION OF THE CAPACITANCE MATRIX METHOD TO ACCOMMODATE MASKED LAND AREAS AND ISLAND CIRCULATIONS IN A PRIMITIVE EQUATION OCEAN MODEL

JOHN L. WILKIN AND JAMES V. MANSBRIDGE

CSIRO Division of Oceanography, GPO Box 1538, Hobart, Tasmania 7001, Australia

AND

KATHERINE S. HEDSTRÖM

Institute of Marine and Coastal Sciences, Rutgers University, PO Box 231, New Brunswick, NJ 08903, U.S.A.

SUMMARY

The capacitance matrix method has been implemented in a primitive equation ocean model to accommodate islands and portions of irregular coastal boundaries that cannot be treated adequately by boundary-fitted orthogonal curvilinear co-ordinates. The algorithm preserves the ability to solve the streamfunction equation using fast and accurate elliptic solvers that require a rectangular computational domain. By superposition of a set of island Green functions, the solution is adjusted to ensure continuity of pressure around each island. The implementation is tested by comparison with an analytic solution for wind-driven flow in a closed basin similar to the southwest Pacific Ocean.

KEY WORDS capacitance matrix; elliptic equation; Green function; multigrid; ocean model

1. INTRODUCTION

A new diabatic primitive equation model for studying regional and basin-scale ocean circulation processes has been described by Haidvogel *et al.*[1] The model employs a 'sigma' bathymetry-following co-ordinate transformation in the vertical and a spectral vertical discretization procedure in which the structure of the model variables is represented as an expansion in a finite set of continuous basis functions. In the horizontal, boundary-fitted orthogonal curvilinear co-ordinates map moderately irregular lateral boundaries to a rectangular computational domain and the model equations are discretized using centred finite differences. Employing a horizontal mapping that retains a rectangular computational domain makes the code efficient on vector-processing computers and allows the use of fast and accurate algorithms for the solution of the two-dimensional elliptic boundary value problem governing the depth-integrated mass transport or streamfunction.

Available fast elliptic solvers generally accommodate singly or doubly periodic, mixed derivative and specified (Dirichlet) boundary conditions, but these boundary conditions must be applied on the edges of a rectangular computational domain. Thus the present formulation of the Haidvogel *et al.*[1]

CCC 0271–2091/95/070662–14

Received January 1994
Accepted October 1994

semispectral primitive equation model (SPEM) can be applied directly to ocean basins whose irregular boundaries can be represented adequately by the boundary-fitted orthogonal co-ordinates, including basins with singly or doubly periodic open boundaries.

A feature of ocean regions that cannot be accommodated by the above elliptic solvers and boundary condition schemes is the inclusion of islands within the model domain. This requires the imposition of additional constraints on the streamfunction along contours within the computational domain. Also, in some applications with highly irregular lateral boundaries, orthogonal curvilinear boundary-fitted co-ordinates will have large variations in physical grid spacing. There comes a trade-off between maintaining adequate horizontal resolution in regions where the grid spacing is large and creating regions of fine grid spacing that place a severe limitation on the model time step.[2] In such situations it may be desirable to 'mask' certain regions of the computational domain that correspond to land areas in the physical domain in order to give greater flexibility in the generation of the boundary-fitted co-ordinates. This situation also requires the imposition of additional boundary conditions on the streamfunction within the computational domain.

The capacitance matrix method (CMM), so-named for its initial application in classical potential problems,[3,4] is an algorithm for imposing additional conditions on the solution of a boundary-value elliptic problem at specified grid points in the interior of the computational domain. The algorithm effectively determines a modification to the right-hand side of the governing elliptic equation which will precisely satisfy the additional interior 'boundary' conditions. The algorithm has the advantage of retaining the ability to use fast and accurate elliptic solving subroutines at modest additional computational expense and has been favoured in recent oceanographic applications[5,6] for this reason.

A brief summary of the primitive equations traditionally used in ocean circulation modelling is presented in Section 2, including a derivation of the elliptic equation for the mass transport streamfunction in orthogonal curvilinear co-ordinates. In Section 3 the CMM algorithm for solving the streamfunction equation is described. In problems where the total mass transport through the passages separating islands is not known *a priori*, it is necessary to adjust the solution according to the net circulation around each island generated by the model forcing. Section 4 describes the modification of the CMM solution required to allow for such island circulation by the superposition of a set of island Green functions. Finally, Section 5 presents an application of the algorithm to a simulation of the circulation in the subtropical gyre of the South Pacific where the flow is affected by the presence of islands.

2. PROBLEM FORMULATION

2.1. The primitive equations

In diabatic large- and regional-scale ocean circulation modelling it is traditional to solve the so-called primitive equations (e.g. Reference 7) derived from the Navier–Stokes equations under the Boussinesq and hydrostatic approximations. The Boussinesq approximation assumes that density variations do not contribute to the momentum balance except in the buoyancy force, which under the hydrostatic approximation is balanced solely by the vertical pressure gradient. The primitive equations may be written as

$$\frac{\partial \mathbf{u}}{\partial t} + (\mathbf{u} \cdot \nabla)\mathbf{u} + w\frac{\partial \mathbf{u}}{\partial z} + f\mathbf{k} \times \mathbf{u} = -\frac{1}{\rho_o}\nabla p + \mathbf{F}_\mathbf{u} + \mathbf{D}_\mathbf{u}, \tag{1}$$

$$\rho g = -\frac{\partial p}{\partial z}, \tag{2}$$

$$\nabla \cdot \mathbf{u} + \frac{\partial w}{\partial z} = 0, \tag{3}$$

$$\frac{\partial T}{\partial t} + \mathbf{u} \cdot \nabla T + w\frac{\partial T}{\partial z} = F_T + D_T, \tag{4}$$

$$\frac{\partial S}{\partial t} + \mathbf{u} \cdot \nabla S + w\frac{\partial S}{\partial z} = F_S + D_S, \tag{5}$$

where $\mathbf{u}$ is a vector of the horizontal velocity components, w is the vertical (z) velocity, ρ_o is a constant background density, $\rho_o + \rho$ is the total density and f is the Coriolis parameter. Equation (1) expresses conservation of horizontal momentum, (2) vertical momentum, (3) mass, (4) temperature and (5) salt. T and S are related to ρ through an equation of state. Forcing and dissipation are represented schematically by the terms F and D.

2.2. *Orthogonal curvilinear horizontal co-ordinates*

In ocean-modelling applications the region of interest is frequently confined within irregular lateral boundaries. An efficient method of incorporating moderately irregular horizontal geometry is to use a boundary-fitted orthogonal co-ordinate system. For general orthogonal horizontal co-ordinates ξ and η, physical arc lengths ds_ξ and ds_η and elemental distances $d\xi$ and $d\eta$ are related by $ds_\xi = (1/m)d\xi$ and $ds_\eta = (1/n)d\eta$, where m and n are the metric coefficients of the co-ordinate system.[8] Metric coefficients for arbitrarily shaped domains can be computed efficiently by conformally mapping the lateral boundaries to a rectangle and filling in the interior grid points by solving Laplace's equation.[9] By using appropriate angle-conserving map projections, a grid computed by this procedure in Cartesian co-ordinates can be mapped to the surface of a sphere to produce orthogonal co-ordinates suitable for large-scale ocean-modelling problems.[2]

Using boundary-fitted co-ordinates also provides a method for increasing the computational resolution in areas of particular interest where this is advantageous for an accurate solution. For example, Figure 1 shows the co-ordinate grid used in the test simulations described in Section 5. The grid has relatively high resolution along the Australian cast which improves the simulation of the oceanic western boundary current, and lower resolution in the east where this is adequate for simulating the large-scale circulation of the subtropical gyre.

2.3. *Mass transport streamfunction*

Denoting a vertical average by an overbar, equation (1) may be written as

$$\frac{\partial \bar{\mathbf{u}}}{\partial t} = \bar{\mathbf{R}}_\mathbf{u} - \frac{1}{\rho_o}\nabla p_s, \tag{6}$$

where the vector $\mathbf{R}_\mathbf{u}$ represents all terms in the horizontal momentum balance except the gradient of the surface pressure p_s. Taking the curl of (6) gives

$$\frac{\partial Z}{\partial t} = \nabla \times \bar{\mathbf{R}}_\mathbf{u}, \tag{7}$$

where

$$Z = \nabla \times \bar{\mathbf{u}} \tag{8}$$

is the depth-averaged vorticity.

By assuming that the depth-averaged flow is horizontally non-divergent (the rigid lid

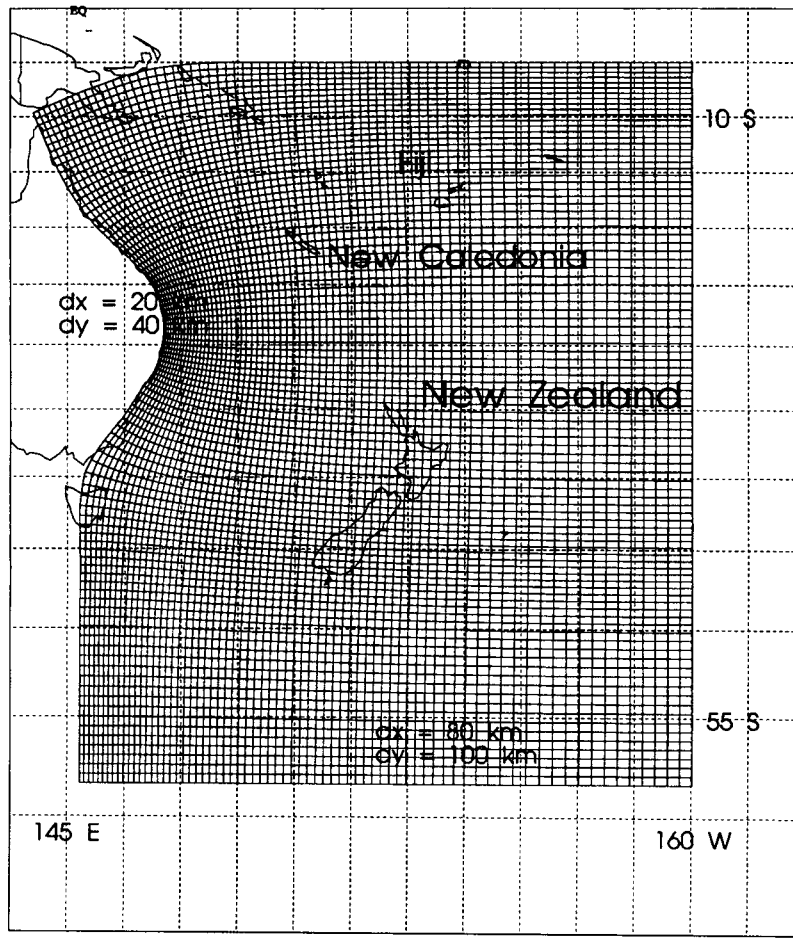

Figure 1. Orthogonal curvilinear grid fitted to the coastal boundaries of the southwest Pacific used in the example simulation in Section 5. Grid resolution varies from Δx = 20 km, Δy = 40 km near 30° S on the Australian coast to Δx, $\Delta y \approx 100$ km in the east of the domain

approximation), a streamfunction Ψ may be defined via

$$\bar{u} = -\frac{n}{h}\frac{\partial \Psi}{\partial \eta}, \qquad \bar{v} = \frac{m}{h}\frac{\partial \Psi}{\partial \xi}, \tag{9}$$

where u and v are the components of velocity in the directions ξ and η respectively and h is the depth. In orthogonal co-ordinates the vertical component of the curl of any vector $\mathbf{A}$ is

$$(\nabla \times \mathbf{A})_z = mn\left[\frac{\partial}{\partial \xi}\left(\frac{A_\eta}{n}\right) - \frac{\partial}{\partial \eta}\left(\frac{A_\xi}{m}\right)\right]. \tag{10}$$

Then substituting (9) into (8) gives the elliptic equation governing Ψ in orthogonal curvilinear co-ordinates as

$$\frac{m}{hn}\frac{\partial^2 \Psi}{\partial \xi^2} + \frac{n}{hm}\frac{\partial^2 \Psi}{\partial \eta^2} + \frac{\partial}{\partial \xi}\left(\frac{m}{hn}\right)\frac{\partial \Psi}{\partial \xi} + \frac{\partial}{\partial \eta}\left(\frac{n}{hm}\right)\frac{\partial \Psi}{\partial \eta} = Z. \tag{11}$$

2.4. Numerical solution

In practice, at each model time step the right-hand side of (11) is determined by integrating with respect to time the prognostic equation (7) for Z. Then the solution to (11) is fully prescribed by specifying values for Ψ on the boundary.

Many algorithms exist for solving numerically boundary value elliptic problems such as (11). In ocean models using finite differences of fixed spacing in Cartesian or spherical co-ordinates with irregular lateral boundaries accommodated by 'staircase' boundaries, (11) is frequently solved by relaxation methods such as successive overrelaxation (SOR) or preconditioned conjugate gradient (PCG) (e.g. Reference 10). SOR can be prone to gradual instabilities and poor convergence in some situations[11] and more accurate algorithms are preferred if they are available. Blayo and Le Provost[6] have implemented the CMM in concert with a Fourier analysis–cyclic reduction (FACR) fast Helmholtz equation solver to accommodate irregular coastal boundaries (but not islands) in a quasi-geostrophic ocean model. They found that the CMM–FACR combination retains the accuracy of the FACR method in a rectangular domain (relative error of order 10^{-8}) and that CMM–FACR performed 11·5 times faster than PCG taken to comparable accuracy and three times faster than PCG taken to order 10^{-3} accuracy.

In SPEM applications where a simple idealized geometry (namely, constant depth and metric coefficients m and n not functions of η and ξ (respectively) renders (11) separable, fast direct solvers from the FISHPAK library of FORTRAN subroutines[12] have been used for the solution. In general applications where the elliptic equation is not separable or the memory demands of a direct solver are prohibitive, an elliptic solver based on the multigrid method from the MUDPACK library[13] has been favoured.

The FISHPAK and MUDPACK elliptic solvers accommodate singly or doubly periodic, mixed derivative and specified (Dirichlet) boundary conditions, but these boundary conditions must be applied on the edges of the rectangular computational domain. In order to extend these algorithms to accommodate masked land areas contiguous to the perimeter of the domain or islands within the domain, modifications to the procedure for solving (11) are required. The CMM is one such algorithm.

3. THE CAPACITANCE MATRIX ALGORITHM

The capacitance matrix method is described fully here with slightly varied notation from that of Milliff,[5] because there are several differences between the present problem formulation and Milliff's with respect to boundary conditions and the inclusion of island circulation.

3.1. Problem statement

The notation describing the subregions and boundaries of the computational domain is depicted in Figure 2. The full domain is denoted Ω and is comprised of subdomains Ω_O, the *ocean* region, Ω_M, the *mainland* (which is any land area contiguous to the perimeter), and Ω_I, the *islands*. The perimeter of the computational domain is denoted δ and is comprised of δP, the *perimeter* of the ocean region, and δE, the *exterior* of the mainland region. Land regions are separated from the ocean by boundaries δM of the *mainland* region and δI for the *islands*. There will be N_I of the Ω_I subdomains and δI boundaries, one for each of the N_I islands. In addition, δC denotes all *coastlines* within the interior of the computational domain, i.e. $\delta C = \delta M + \sum_{I=1}^{N_I} \delta I$, and δO denotes the physical boundary of the multiply connected *ocean*, i.e. $\delta O = \delta P + \delta C$.

The elliptic problem to be solved may be stated as

$$\mathscr{L}\Psi = Z \tag{12}$$

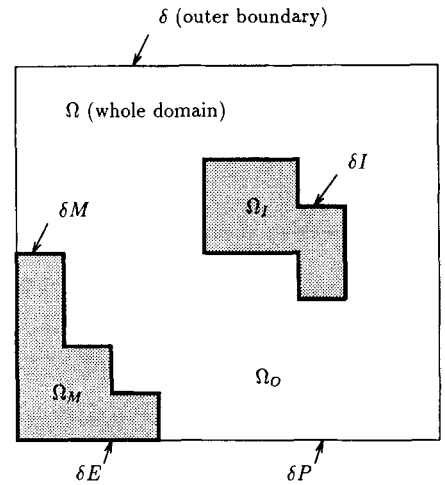

Figure 2. Schematic of the subregions and boundaries of the computational domain

in the region Ω_O subject to $\Psi(\delta O)$ prescribed. Here $\mathscr{L}$ is the two-dimensional differential operator corresponding to (11). In applications where there are no mainland or island areas to be masked, i.e. $\delta O = \delta P$, (12) can be solved numerically with a fast elliptic solver of the class discussed above. In applications where there are land regions to be masked, the CMM is employed to enforce prescribed values of Ψ along δC.

3.2. *Discrete formulation*

The convention followed so far is that two-dimensional variables that are continuous functions of the horizontal co-ordinates (ξ, η) are written as uppercase Greek or Roman characters, e.g. Ψ, Z. When these are discretized onto the numerical grid as 2D matrices, they will be denoted in boldface, e.g. $\boldsymbol{\Psi}$, **Z**. Vectors corresponding to discrete subsets of 2D fields, such as $\boldsymbol{\Psi}$ along a coastline boundary, will be denoted by superscripted lowercase characters. For example, $\psi^{\delta M}$ denotes the values of $\boldsymbol{\Psi}$ at the grid points defining the mainland boundary δM. Operators that project the 2D fields onto these boundary node vectors will be indicated in superscripted uppercase. For example, the boundary projection operator that returns the values of $\boldsymbol{\Psi}$ along δM is denoted $B^{\delta M}$ and thus

$$B^{\delta M}\boldsymbol{\Psi} \equiv \psi^{\delta M}. \tag{13}$$

Defining L to be the discrete analogue of the differential operator $\mathscr{L}$ in (12), the problem is to find a solution to

$$L\boldsymbol{\Psi} = \mathbf{Z} \tag{14}$$

in the region Ω_O that satisfies boundary conditions on $\psi^{\delta O}$. The boundary conditions will be a combination of Ψ = constant on solid land boundaries and, where δP is ocean, open boundary conditions that could be any of singly or doubly periodic, mixed derivative or prescribed (according to e.g. a radiation condition). The boundary conditions on the interior coastlines, namely $\psi^{\delta C}$, will be denoted here by a vector **b**. Typically Ψ on the mainland and ocean perimeter is assigned a constant

value k_0 and Ψ on each island individual constant values k_I. Then $\mathbf{b}$ will be of the form

$$\mathbf{b} = \begin{pmatrix} k_0\mathbf{e}_M \\ k_1\mathbf{e}_1 \\ \vdots \\ k_I\mathbf{e}_I \\ \vdots \\ k_{N_I}\mathbf{e}_{N_I} \end{pmatrix}, \tag{15}$$

where each $\mathbf{e}$ is a vector of ones of length the number of boundary nodes defining that section of coastline, whether it be mainland (M) or island (I). The boundary conditions on (14) along δC may then be written as

$$\psi^{\delta C} = \mathbf{b}. \tag{16}$$

Prescribing the k_I is equivalent to stating that the mass transport between each island is known *a priori*. The situation in which the k_I evolve with time is treated in Section 4.

3.3. *Implementation*

The CMM obtains the solution to (14) in two steps. First a *particular* solution Ψ_P is obtained which satisfies vorticity forcing and boundary conditions on the perimeter of the computational domain. Then a *homogeneous* solution Ψ_H is obtained and superposed with Ψ_P so that the final solution $\Psi = \Psi_P + \Psi_H$ also satisfies the boundary conditions on the interior coastlines δC.

3.3.1. *Particular solution.*

Computing Ψ_P is straightforward. It is the solution to

$$L\Psi_P = \mathbf{Z} \tag{17}$$

in the region Ω that satisfies the perimeter boundary conditions, i.e. $\psi_P^\delta = \psi^\delta \equiv B^\delta\Psi$. This solution is obtained by direct application of a fast elliptic solver. The values of $\mathbf{Z}$ in the land regions $\left(\Omega_M + \sum_{I=1}^{N_I} \Omega_I\right)$ and of $\psi_P^{\delta E} \equiv B^{\delta E}\Psi_P\}$ are arbitrary and may be taken as zero.

3.3.2. *Homogeneous solution.*

Let $\mathbf{Z}_{G_n}$ be a vorticity-forcing function having unit value on boundary node n of δC and zero value everywhere else. Then Ψ_{G_n} is the *influence function* for node n and satisfies

$$L\Psi_{G_n} = \mathbf{Z}_{G_n} \tag{18}$$

in Ω subject to $\psi_{G_n}^\delta \equiv B^\delta\Psi_{G_n} = 0$ (i.e. homogeneous boundary conditions) or periodic conditions if these are being applied on any part of δP. Equation (18) is solved with a fast elliptic solver. Ψ_{G_n} is effectively a discrete Green function for boundary node n. There will be N_B such functions, where N_B is the number of grid points defining δC. The homogeneous solution is a weighted sum of influence functions, i.e.

$$\Psi_H = \sum_{n=1}^{N_B} \Psi_{G_n} w_n, \tag{19}$$

where the weights w_n are to be determined so as to enforce the additional boundary conditions on δC. Note that the vorticity sources are located *on* the boundary δC and do not fall within the region Ω_O. This ensures that $L\,\Psi_H = 0$ in Ω_O and the superposition of the solutions Ψ_H and Ψ_P still satisfies (14).

Applying the boundary node projection operator for the interior coastlines ($B^{\delta C}$) to (19) gives

$$\psi_{\mathrm{H}}^{\delta C} \equiv B^{\delta C}\Psi_{\mathrm{H}} = \sum_{n=1}^{N_B} B^{\delta C}\Psi_{G_n} w_n. \tag{20}$$

Forming a matrix $\mathbf{K}$ whose columns are $B^{\delta C}\Psi_{G_n}$, and denoting a vector of the weights w_n by $\mathbf{w}$, (20) may be written as

$$\psi_{\mathrm{H}}^{\delta C} = \mathbf{K}\mathbf{w}. \tag{21}$$

From the superposition of particular and homogeneous solutions it is required that the boundary conditions (16) along δC are

$$\psi_{\mathrm{P}}^{\delta C} + \psi_{\mathrm{H}}^{\delta C} = \mathbf{b}. \tag{22}$$

Substituting (21) into (22) and rearranging, a solution is obtained for the influence function weights:

$$\mathbf{w} = \mathbf{K}^{-1}\left(\mathbf{b} - \psi_{\mathrm{P}}^{\delta C}\right). \tag{23}$$

$\mathbf{K}^{-1}$ is referred to as the *capacitance matrix*. At each model time step the matrix multiplication (23) must be performed to evaluate $\mathbf{w}$. However, it is impractical to store the N_B influence functions Ψ_{G_n} and multiply these by $\mathbf{w}$ to get Ψ_{H} at every model time step. Rather, the right-hand side of (14) is augmented with a vorticity-forcing field

$$\mathbf{Z}_{\mathrm{H}} = \sum_{n=1}^{N_B} \mathbf{Z}_{G_n} w_n \tag{24}$$

consisting of the weights w_n distributed along the boundary δC. Then the solution to

$$L\Psi = \mathbf{Z} + \mathbf{Z}_{\mathrm{H}} \tag{25}$$

in Ω subject to boundary conditions ψ^{δ} will be precisely $\Psi_{\mathrm{P}} + \Psi_{\mathrm{H}}$. Equation (25) can be solved directly with a fast elliptic solver, because the boundary conditions are prescribed only on the perimeter of the computational domain δ.

3.4. Computational considerations

The solution procedure effectively finds the vorticity field $\mathbf{Z}_{\mathrm{H}}$ that added to the right-hand side of (14) produces a solution that satisfies the boundary conditions on the interior coastlines. In the absence of any interior coastal boundaries (i.e. $\delta = \delta O$) Ψ_{P} would be the complete solution for the streamfunction. At each model time step the additional computational expense in applying the capacitance matrix method when interior boundaries are present is the evaluation of the matrix product (23) and the re-evaluation of the elliptic solution with the new vorticity forcing $\mathbf{Z} + \mathbf{Z}_{\mathrm{H}}$. There is also an additional step at initialization. The capacitance matrix $\mathbf{K}^{-1}$ depends on the influence functions for the particular problem, which do not alter as the solution evolves in time. Thus the Ψ_{G_n} are calculated once at initialization by the fast elliptic solver and the matrix $\mathbf{K}$ evaluated, inverted and stored. $\mathbf{K}^{-1}$ has as dimension the number of grid points defining the discretized interior coastlines (N_{B}), which might typically be of the order of 100 points. Our experience with the SPEM is that the initialization overhead and the multiplication (23) are insignificant and the second elliptic solve at each time step increases the computation time by about 30 per cent. This is for model resolutions of the order of 100×100 grid points and seven vertical modes. For higher vertical resolution the overhead will be proportionately less, because the streamfunction calculation is independent of vertical resolution.

We emphasize here that the CMM is quite general and can be used with fast elliptic solver subroutine libraries because it modifies only the right-hand side of the elliptic problem. An alternative approach to enable the use of a fast multigrid solver was adopted by Jensen,[14] who developed several

strategies for interpolating the masked land region to the differing resolution grids at each level of the multigrid iteration cycle. The interior boundary conditions were imposed by tracking land points and setting the streamfunction value explicitly during each iteration.

4. MODIFYING THE SOLUTION TO ALLOW FOR AROUND-ISLAND CIRCULATION

In Section 3.2 it was assumed that k_I, the value of Ψ on each island, could be specified *a priori*. In general this is seldom the case, since the transport between the islands evolves with time in response to the forcing and is determined by the condition that the surface pressure must be continuous, following any closed path around each island.

A consequence of the rigid lid approximation is that the surface pressure p_s is not carried explicitly in the model. Therefore its effect on the circulation around each island is inferred by a line integration of the depth-averaged momentum balance. Around any closed path $\mathbf{s}$

$$\oint \nabla p_s \cdot d\mathbf{s} = 0 \tag{26}$$

which implies from (6) that

$$\frac{\partial \Gamma_I}{\partial t} = \oint_I \bar{\mathbf{R}}_\mathbf{u} \cdot d\mathbf{s}, \tag{27}$$

where

$$\Gamma_I = \oint_I \bar{\mathbf{u}} \cdot d\mathbf{s} \tag{28}$$

is the circulation following the chosen path around island I. Equation (27) is integrated at each time step to give Γ_I for each island at the new time level.

Let $\hat{\Psi}$ denote the solution to (25) obtained by the CMM and $\hat{\Gamma}_I$ the corresponding island circulation values. Substitution of (9) into (28) gives

$$\hat{\Gamma}_I = \oint_I -\frac{1}{h}\frac{\partial \hat{\Psi}}{\partial r}\, ds, \tag{29}$$

where r is an inward-directed normal to the path of integration. The discrepancy between Γ_I and $\hat{\Gamma}_I$ can be amended by adding to $\hat{\Psi}$ a weighted sum of island Green functions Ψ_I, defined as the solution to

$$\mathscr{L}\Psi_I = 0 \tag{30}$$

in Ω_O subject to $\Psi_I = 1$ on island I, zero on all other islands and the mainland and either zero or periodic conditions on the appropriate portions of the perimeter. Here $\mathscr{L}$ is the same operator as in (12), so the Ψ_I are readily computed by the procedure described in Section 3.

A weighted sum of Ψ_I will add

$$\Gamma_I^* = \sum_{J=1}^{N_I} w_J^* C_{I,J} \tag{31}$$

to the circulation around island I, where w_J^* are the weights and

$$C_{I,J} = \oint_I -\frac{1}{h}\frac{\partial \hat{\Psi}_J}{\partial r}\, ds \tag{32}$$

is the circulation induced around island I due to Ψ_J. Adopting vector notation, the circulation that must

be added to the present solution is $\Gamma - \hat{\Gamma}$ and therefore the required set of weights is given by

$$\mathbf{w}^* = \mathbf{C}^{-1}(\Gamma - \hat{\Gamma}), \tag{33}$$

where the island interaction matrix C^{-1} is the inverse of a matrix with elements $C_{I,J}$.

The complete solution allowing for island circulation is then

$$\Psi = \hat{\Psi} + \sum_{I=1}^{N_I} w_I^* \Psi_I. \tag{34}$$

This adjustment is applied only to islands for which the streamfunction is unknown *a priori*. For these islands the constant streamfunction boundary conditions k_I introduced in (15) are arbitrary and may be taken as zero.

The Ψ_I are dependent only upon the model geometry and may be computed once at model initialization and stored. For example, the Green functions for the three islands in the southwest Pacific test case in the next section are shown in Figure 3. The island interaction matrix C^{-1} is similarly computed only once and stored.

In other ocean models[7,14,15] the circulation condition (27) is used to form an equation similar to (33) but for the values of Ψ itself on the islands. The island Ψ-values are then explicitly included in the discretization (e.g. SOR, PCG or multigrid) of the governing equation at each iteration of the solution procedure.

5. EXAMPLE

As an example of the performance of the CMM in the SPEM, we present the results of wind-driven ocean circulation simulations in an idealized representation of the Tasman and Coral Sea region of the southwest Pacific Ocean (Figure 1). All the perimeter boundaries are closed and the basin has a uniform depth of 2000 m. Steady wind forcing is applied that is similar in strength to the annual mean east–west component of wind stress observed in the central South Pacific. No north–south component of wind stress and surface fluxes of heat or salt are applied. Initially the ocean is at rest and the vertical temperature and salt stratification is similar to the observed profiles averaged over the region. Simulations have been conducted with and without the islands of New Zealand, New Caledonia and Fiji to illustrate the effect of these islands on the wind-driven circulation. A test of the CMM is provided by comparing the model streamfunction with that computed from a simple Sverdrup calculation using linear wind-driven dynamics and the 'island rule' of Godfrey.[16]

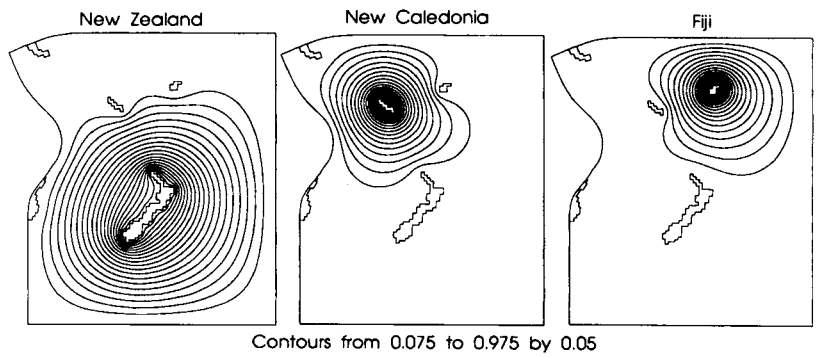

Figure 3. Green functions Ψ_I for the three islands in the southwest Pacific example

The Sverdrup solution assumes a steady balance between the wind stress and the Coriolis force acting on the depth-integrated transport in an ocean of uniform depth. This balance produces a circulation in the ocean interior that is equatorward (poleward) in regions of positive (negative) curl of the wind stress. Friction is assumed to play a role only in boundary currents that close the transport of the interior circulation.

Figure 4(a) shows the Sverdrup circulation in the closed basin geometry of Figure 1 for the given latitudinal distribution in wind stress. Negative contours indicate a counterclockwise sense to the circulation. The closure of these contours along the western, northern and southern boundaries is not shown, since this closure is assumed to occur in boundary currents of arbitrarily small width. Figure 4(b) shows the effect of including the three islands. The islands interrupt the westward propagation of Rossby waves and lead to the formation of boundary currents on the east coast of each island, with a consequent weakening of the boundary current on the western boundary of the basin. This is most pronounced for New Zealand, where mainland and island boundary currents are connected by an east–west jet at the latitude of the northern tip of New Zealand.

Figure 5 shows the corresponding model solutions at day 1000 when the model momentum equations are linearized, lateral friction is kept small and bottom friction is zero, to make the model dynamics as close as possible to the Sverdrup solution approximations. In both cases the solutions are very similar to the Sverdrup solution, especially in the ocean interior. In the model the narrow frictional boundary currents are resolved and show that water leaving the western boundary current moves slightly northward before joining the interior Sverdrup circulation. This feature of the circulation is known from analytic solutions to the barotropic vorticity equation by Munk[17] when a no-stress lateral boundary condition is applied along the coast.

The CMM successfully achieves a constant streamfunction along each island coastline to within a relative error of typically 10^{-6}. For the case of New Zealand this corresponds to a maximum mass sink or source at the coast of less than 2 $m^3\ s^{-1}$.

The streamfunction values on the three islands for the model solution are compared with the 'island rule' solution in Figure 6. The model solution varies in time owing to transients generated when starting the model abruptly from rest. These are not damped appreciably because of the very weak lateral friction applied in order to duplicate the inviscid Sverdrup solution case as closely as possible.

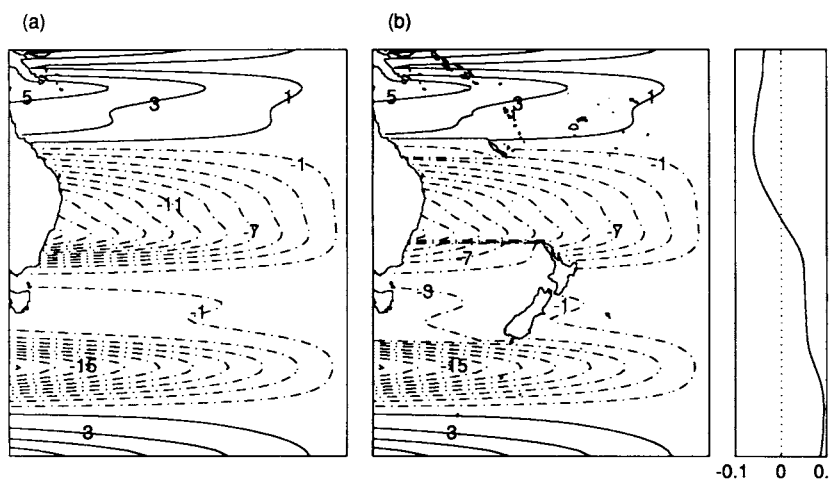

Figure 4. Streamfunction solution predicted by Sverdrup dynamics for wind-driven flow in an idealized ocean basin analogous to the southwest Pacific. The latitudinal profile of wind stress is shown on the right in Pascals. (a) Without and (b) with the presence of the islands of New Zealand, New Caledonia and Fiji. Contour interval is $2 \times 10^6\ m^3\ s^{-1}$

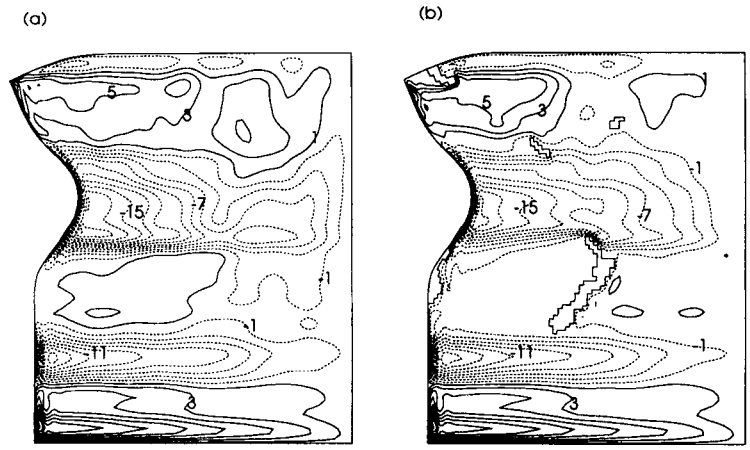

Figure 5. For linear model dynamics, the streamfunction after 1000 days for the cases corresponding to Figure 4

Nevertheless, it is evident that the mean island streamfunction values are close to the Sverdrup solution values, indicating that the island Green function adjustment of the CMM solution achieves the correct transport between islands.

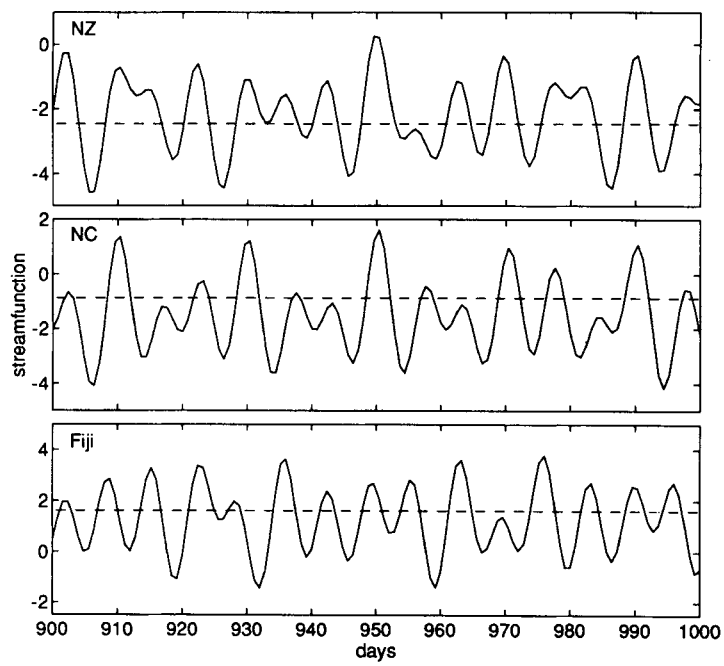

Figure 6. Solid curves: streamfunction ($\times 10^6$ m^3 s^{-1}) on islands of New Zealand (NZ), New Caledonia (NC) and Fiji in southwest Pacific test case for days 900–1000 of simulation. Broken lines: corresponding solutions from Sverdrup dynamics 'island rule'

6. CONCLUSIONS

The capacitance matrix method has been implemented in the SPEM to allow the inclusion of masked areas of land such as islands and coastal promontories. Used in conjunction with the SPEM's boundary-fitted orthogonal curvilinear co-ordinates, the method enables the efficient use of fast and accurate (e.g. multigrid) algorithms that require a rectangular computational domain when solving the elliptic equation governing the streamfunction.

The requirement that the surface pressure field be continuous, following any closed path in the ocean, applies a constraint on the circulation around each island that must be satisfied at each model time step. This is handled by superposing with the CMM solution a set of island Green functions whose amplitudes are determined by solution of an island interaction equation.

The initialization and island interaction steps of the method impose minimal additional computational cost. The necessity for a second application of the fast elliptic solver at each time step adds approximately 30 per cent to the model execution time for typical three-dimensional ocean circulation problems.

The implementation has been tested successfully by comparing the model and an analytic solution for wind-driven flow in an ocean domain similar to the southwest Pacific that includes three islands.

ACKNOWLEDGEMENTS

We thank D. B. Haidvogel and R. F. Milliff for helpful discussions on addressing the problem of masking land areas in SPEM. J. S. Godfrey assisted in formulating the southwest Pacific test case. J.L.W. and J.V.M. are funded by Australia's National Greenhouse Research Program.

APPENDIX: ACCESS TO THE SPEM SOURCE CODE

The Fortran source code for the SPEM,[1] which includes the CMM implementation described here, is freely available over Internet by anonymous ftp (user ftp, e-mail address as password) to host ahab.rutgers.edu (IP number 128.6.142.5) in directory pub/spem/src. The formulation and configuration of the model are described in detail in the SPEM user's manual.[18]

REFERENCES

1. D. B. Haidvogel, J. L. Wilkin and R. Young, 'A semi-spectral primitive equation ocean circulation model using vertical sigma and orthogonal curvilinear horizontal coordinates', *J. Comput. Phys.*, **94**, 151–184 (1991).
2. J. L. Wilkin and K. S. Hedstrom, 'Orthogonal grid generation for ocean models', unpublished manuscript, 1992.
3. R. W. Hockney, 'The potential calculation and some applications', *Methods Comput. Phys.*, **9**, 135–211 (1970).
4. W. Proskurowski and O. Widlund, 'On the numerical solution of Helmholtz's equation by the capacitance matrix method', *Math. Comput.*, **30**, 433–468 (1976).
5. R. F. Milliff, 'A modified capacitance matrix method to implement coastal boundaries in the Harvard open ocean model', *Math. Comput. Simul.*, **31**, 541–564 (1990).
6. E. Blayo and C. Le Provost, 'Performance of the capacitance matrix method for solving Helmholtz-type equations in ocean modelling', *J. Comput. Phys.*, **104**, 347–360 (1993).
7. K. Bryan, 'A numerical method for the study of the circulation of the world ocean', *J. Comput. Phys.*, **4**, 347–376 (1969).
8. A. Arakawa and V. R. Lamb, 'Computational design of the basic dynamical processes of the UCLA general circulation model', in J. Chang (ed.), *Methods in Computational Physics*, Vol. 17, Academic, New York, 1977, pp. 173–265.
9. D. C. Ives and R. M. Zacharias, 'Conformal mapping and orthogonal grid generation', *AIAA Paper 87-2057*, 1987.
10. E. L. Poole and J. M. Ortega, 'Multicolor ICCG methods for vector computers', *SIAM J. Numer. Anal.*, **24**, 1394–1418 (1987).
11. P. D. Killworth and J. M. Smith, 'Gradual instability of relaxation–extrapolation schemes', *Dyn. Atmos. Oceans*, **8**, 185–213 (1984).
12. P. N. Swartztrauber and R. A. Sweet, 'Efficient Fortran subprograms for the solution of separable elliptic partial differential equations', *ACM Trans. Math. Softw.*, **5**, 352–364 (1979).

13. J. Adams, 'MUDPACK: Multigrid Fortan software for the efficient solution of linear elliptic partial differential equations', *Appl. Math. Comput.*, **34**, 113–146 (1989).
14. T. G. Jensen, 'Application of multi-level techniques to the Stommel problem with irregular boundaries', in J. J. O'Brien (ed.), *Advanced Physical Oceanographic Modelling*, Reidel, Dordrecht, 1986, pp. 87–109.
15. A. J. Semtner, Jr., 'An oceanic general circulation model with bottom topography', *Technical Report 9*, Department of Meteorology, University of California, Los Angeles, CA, 1974.
16. J. S. Godfrey, 'A Sverdrup model of the depth-integrated flow for the World Ocean allowing for island circulations', *Geophys. Astrophys. Fluid Dyn.*, **45**, 89–112 (1989).
17. W. H. Munk, 'On the wind-driven ocean circulation', *J. Meteorol.*, **7**, 79–93 (1950).
18. K. S. Hedström, 'User's manual for a semi-spectral primitive equation ocean circulation model, version 3.9', *Institute of Marine and Coastal Sciences Contribution 93-23*, Rutgers University, New Brunswick, NJ, 1994.